

A New Empirical Ocean Tide Model for Improved High-Frequency Earth Rotation Variations

Matthias Madzak¹, Sigrid Böhm¹, Johannes Böhm¹, Wolfgang Bosch², Jan Hagedoorn³, Harald Schuh^{3,4}

Abstract We seek to improve the current model for high-frequency Earth rotation variations induced by ocean tides. For empirical models, we derive oceanic currents, which are required for the ocean tidal angular momentum. We use the hydrodynamic FES2012 to derive a preliminary test model and analyze the CONT11 campaign to compare it to the IERS recommended model. We find an improvement for yp at the semi-diurnal frequencies. The xp component agrees to a level of about $10 \mu as$, those from UT1–UTC to a level of about three μas .

Keywords Earth rotation, ocean tides, VLBI analysis, project SPOT

1 Introduction

Accurate a priori models are essential for Very Long Baseline Interferometry (VLBI) analysis to derive precise geodetic parameters. In particular orbit prediction for Global Navigation Satellite Systems (GNSS) requires a model for the effect of ocean tides on Earth rotation in the diurnal and sub-diurnal band. The recommended prediction model of this effect is described in the IERS Conventions 2010, Chapter 8 [1].

However, there are significant differences between the model prediction values and the estimated parameters for polar motion and UT1–UTC. Figure 1 shows those differences for UT1–UTC in the frequency do-

main. The large peaks coincide with the frequencies of the major ocean tides, for example O1 and S1 in the diurnal band and M2 and K2 in the semi-diurnal band.

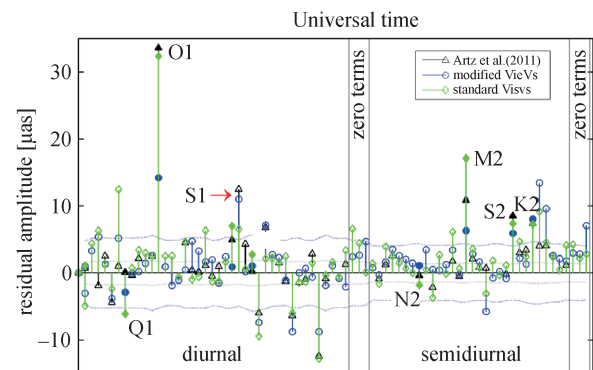


Fig. 1 Spectrum: Residuals of model values and estimated UT1–UTC from VLBI analysis.

The Project SPOT, supported by the Austrian Science Fund (FWF), deals with this issue and seeks to close the gap between model predictions and observations. We develop a new model for high frequency Earth rotation parameter (ERP) variations induced by ocean tides. This could be one step further to meet the GGOS requirements regarding the accuracy of geodetic results (Plag and Pearlman, 2009 [2]).

2 Ocean Tide Models

When using ocean tide models for the calculation of ocean tidal angular momentum (OTAM), there are basically two types of models available. Empirical models, derived solely from satellite altimetry data, include

1. Vienna University of Technology, Austria
2. German Geodetic Research Institute (DGFI), Germany
3. Berlin University of Technology, Germany
4. GeoForschungszentrum Potsdam, Germany

only tidal heights of the ocean surface. Hydrodynamic models, on the other hand, also contain oceanic currents, which are required for the motion term of the angular momentum.

Ocean tide models usually include eight major tides: Q1, O1, P1, and K1 in the diurnal band and N2, M2, S2, and K2 in the semi-diurnal band. Due to the long time span of satellite altimetry observations, it is nowadays possible to estimate further tides in the tidal analysis. The new FES2012 for example includes a total of 27 semi-diurnal and diurnal constituents.

Spatial resolutions of current ocean tide models are 0.125° or even smaller.

3 Worksteps

The workflow to derive a new high-frequency ERP model is shown in Figure 2.

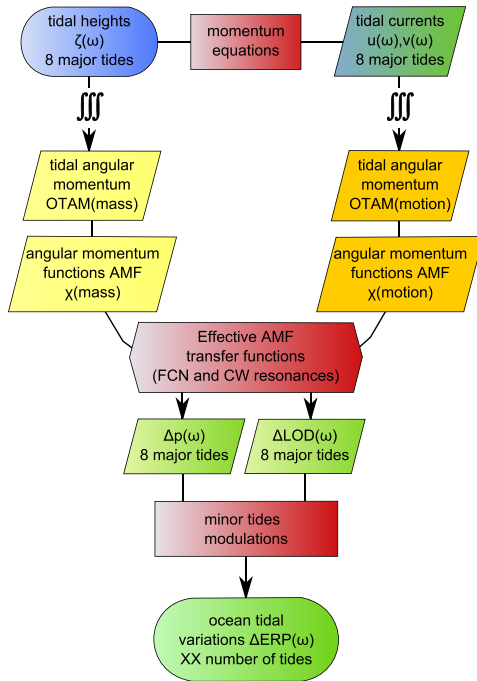


Fig. 2 Workflow of Project SPOT.

The first major task is to derive oceanic currents from tidal heights when an empirical model is used. More details about hydrodynamic equations can be found in Section 4. After numerical integration, we de-

rive ocean tidal angular momentum, both for mass and motion terms.

Time-varying and frequency-dependent OTAM can be converted to ERP using effective angular momentum functions (e.g., Gross, 1993 [3]), which account for Free-Core-nutation and Chandler-wobble resonances.

If minor tides are not included in the ocean tide model, they have to be accounted for during the ERP model derivation using nodal corrections and admittance functions. Lunar tides are affected by the lunar node cycle (18.6 years), which requires amplitude and phase corrections of those tidal constituents [4]. Minor tides can be interpolated using admittance functions: according to Munk and Cartwright (1966) [5], the ratio of the tide generating potential and the tidal height is assumed to be a slowly varying function of frequency. Hence, minor tides can be interpolated from major tides if the tide generating potential is known, e.g., from the Hartmann and Wenzel (1995) tidal potential catalog.

4 Hydrodynamics

The shallow water equations (linearized, simplified, and depth-averaged Navier-Stokes equations) describe the hydrodynamic flow of the ocean. The momentum and continuity equations read (Ray, 2001 [6])

$$\frac{\partial \mathbf{u}}{\partial t} + \mathbf{f} \times \mathbf{u} = -g \nabla (\zeta - \zeta_E - \zeta_s) - \frac{\mathbf{F}}{\rho D}$$

$$\frac{\partial \zeta}{\partial t} = -\nabla \cdot D \mathbf{u},$$

where u is the horizontal velocity vector, f is the Coriolis parameter, g is gravity acceleration, ζ is tidal height, ζ_E is the equilibrium tide, ζ_s is a term accounting for self-attraction and Earth loading, F is bottom friction force, ρ is density, and D is ocean depth.

The parameters, namely horizontal, barotropic tidal oceanic volume transports (velocity multiplied by depth) can be estimated in a least-squares algorithm. Due to the large number of equations, an iterative least-squares solver is advantageous.

Tests of this algorithm were performed using the model HAMTIDE11a, a hydrodynamic model containing (1) tidal heights from which to calculate ocean ve-

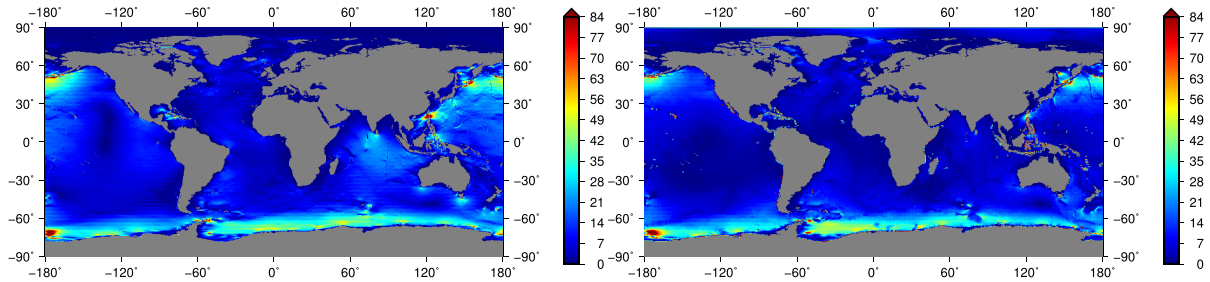


Fig. 3 Volume transport amplitudes (m^2/s) in East direction. Left: Model HAMTIDE11a, right: Estimated from HAMTIDE11a heights using shallow water equations.

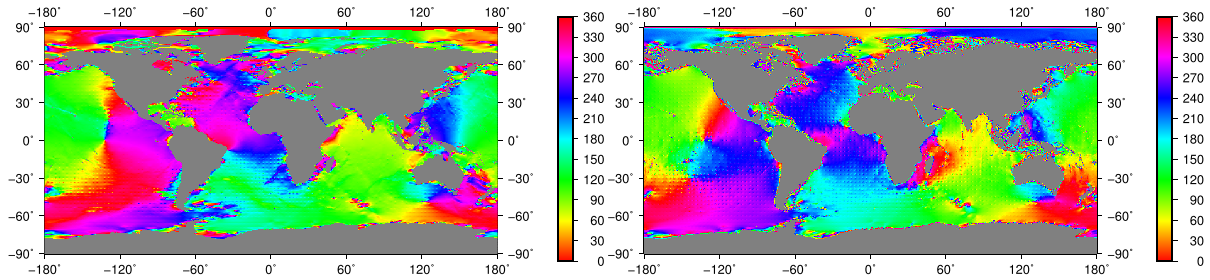


Fig. 4 Volume transport phases ($^\circ$) in East direction. Left: Model HAMTIDE11a, right: Estimated from HAMTIDE11a heights using shallow water equations.

locities and (2) tidal velocities to perform a validation of the estimated results.

Figure 3 shows model values and estimated volume transport amplitudes for the East component.

A similar global pattern can be recognized; differences occur mostly in coastal regions, where no-flow boundaries are used. As expected, the phase (Figure 4) shows larger differences. Likewise the semi-diurnal tides seem to be less accurately estimated.

One possible explanation for problems at different frequencies is the simple friction term in the shallow water equations: $F = r^* \rho u$, where r^* is a friction coefficient. Although there is no physical reason for a frequency-dependent friction coefficient, the simple form of F could absorb other physical mechanisms. Hence, different r^* values for different frequencies might lead to better results.

One possibility of finding the “best” r^* values for each tide is to calculate these coefficients from hydrodynamic model values of tidal heights and currents.

Figure 5 shows the estimated friction parameter values for eight major tides for the models FES2012 and HAMTIDE11a. The diurnal tides seem to have significantly smaller r^* values than the semi-diurnal tides. However, more research needs to be done in this re-

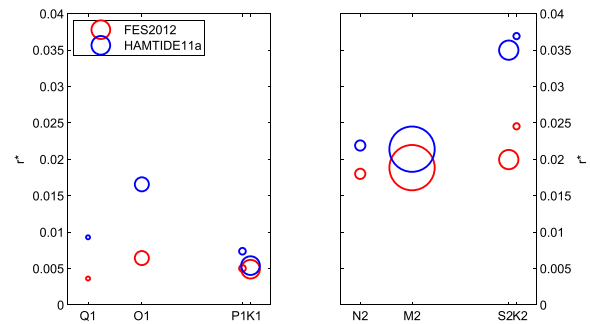


Fig. 5 Estimated friction parameter r^* from hydrodynamic models. The circles are scaled by the tide generating potential of the particular tide.

gard; the results shown in Figures 3 and 4 comprise constant r^* coefficients for all tides.

5 Angular Momentum

Time-varying ocean tidal angular momentum functions are derived for three models. They are summarized in Table 1. The OTAM values of four major constituents

are given in Table 2. The mass terms (height component) agree very well between the two hydrodynamic models (Model A and Model B). The motion terms (current component) are still in good agreement between Model A and Model B. However, Model C shows large differences, especially in phase. It should be noted that diurnal tides show smaller discrepancies than semi-diurnal tides.

Our currents estimated from the shallow water equations are not yet accurate enough to derive an improved ERP model.

Table 1 Overview of models used for the derivation of ocean tidal angular momentum.

Model	Mass term	Motion term
A	FES2012	FES2012
B	HAMTIDE11a	HAMTIDE11a
C	HAMTIDE11a	Estimated*

* Estimated from HAMTIDE11a heights

6 Test Model

Using a hydrodynamic model—and thus not having to calculate oceanic currents—we derive a preliminary test model. We use the FES2012 ocean tide model including a total of 27 tides: six diurnal tides, 13 semi-diurnal tides, and eight tides with even higher frequencies (from one-third to one-eighth of a day). As a numerical integration method, we use Simpson cubature. To convert OTAM to Earth rotation variations, we use the equations and values from Gross (1993) [3].

7 Validation

To validate the test model versus the IERS Conventions 2010 model, we analyze VLBI data from the CONT11 campaign—a 15-day continuous VLBI experiment in September 2011.

In a prior step, we estimate nutation offsets for the time period of CONT11. This is needed, because in the normal parameterization we cannot estimate high-frequency ERP and nutation offsets at the same time. Those nutation offsets dX and dY are used as a priori nutation model for all further processing.

All CONT11 sessions were analyzed using (1) the test model and (2) the IERS Conventions 2010 model

for a priori high-frequency ERP values. For the post-fit residuals of all three ERP, namely x_p , y_p and UT1–UTC, a discrete Fourier transform is calculated. The amplitude spectra were subtracted (“IERS minus test model”), and those spectrum differences allow a validation of the test model: small residuals show a better agreement between observations and the model, and they also yield smaller Fourier coefficients. Because of the order of subtraction (“IERS minus test model”), positive values in the Fourier coefficient differences show a better agreement between the test model and the observations than the IERS model and the observations. Figures 6, 7, and 8 show the Fourier spectrum differences.

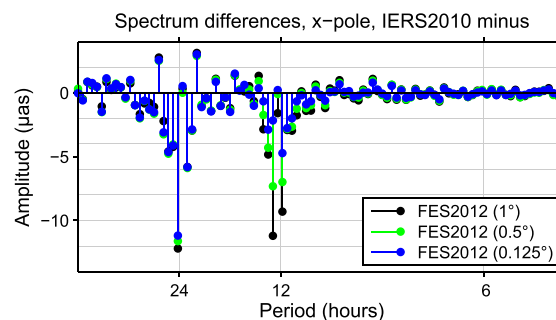


Fig. 6 Fourier spectrum differences between the IERS Conventions 2010 and the test model of the x-pole residuals.

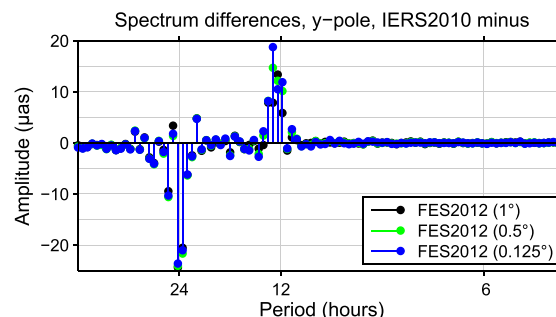
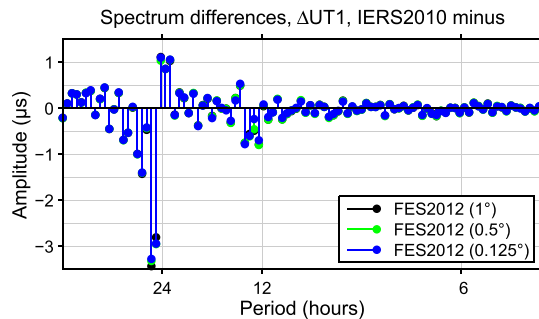


Fig. 7 Fourier spectrum differences between the IERS Conventions 2010 and the test model of the y-pole residuals.

The only improvement compared to the IERS Conventions 2010 model can be seen for y_p at the semi-diurnal frequencies (12-hour period). The semi-diurnal band for x_p and UT1–UTC is of similar accuracy as the IERS model, or slightly worse. Less accurate re-

Table 2 Ocean tidal angular momentum for three models and four major tides. Amplitudes in 10^{25} kg m²/s, phases in degrees.

Tide	Model A				Model B				Model C				
	Heights		Currents		Heights		Currents		Heights		Currents		
K1	x	0.5	-52°	0.6	-71°	0.4	-54°	0.6	-76°	0.4	-54°	0.3	-175°
	y	1.4	-136°	0.8	-168°	1.3	-137°	0.8	-172°	1.3	-137°	0.7	178°
	z	0.2	1°	0.8	128°	0.2	34°	0.7	131°	0.2	34°	0.3	110°
O1		0.5	-30°	0.3	-60°	0.5	-31°	0.3	-60°	0.5	-31°	0.2	133°
		1.2	-138°	0.4	-154°	1.1	-139°	0.4	-155°	1.1	-139°	0.2	177°
		0.2	171°	0.7	115°	0.2	154°	0.5	119°	0.2	154°	0.3	127°
S2		0.1	39°	0.6	-61°	0.1	40°	0.6	-64°	0.1	40°	0.2	89°
		0.3	9°	1.0	-162°	0.3	8°	1.0	-159°	0.3	8°	0.0	-31°
		0.2	132°	0.8	-13°	0.2	132°	0.8	-19°	0.2	132°	0.2	9°
M2		0.5	10°	1.0	-100°	0.5	10°	1.2	-101°	0.5	10°	0.6	37°
		0.3	-56°	1.8	166°	0.3	-58°	1.8	165°	0.3	-58°	0.2	-150°
		0.6	86°	1.5	-45°	0.5	89°	1.7	-41°	0.5	89°	0.6	-13°

**Fig. 8** Fourier spectrum differences between the IERS Conventions 2010 and the test model of the UT1-UTC residuals.

sults can be seen in the 24-hour periods. All three ERP show a better agreement between the IERS Conventions model and the observations than the test model and the observations.

The three figures (6, 7, and 8) show results for the test model in three different spatial resolutions: 1°, 0.5°, and 0.125°. An improvement for higher resolutions can be seen. For example, the values of the 12-hourly xp differences increase from about $-10 \mu\text{as}$ at 1° to about $-5 \mu\text{as}$ at 0.125°.

8 Conclusions

When we use an empirical ocean tide model to derive a new model for high-frequency ERP variations, we need to apply hydrodynamic equations to calculate oceanic currents. Our estimated oceanic currents are not yet accurate enough to be used in an ERP model.

If a hydrodynamic model such as FES2012 is used, results are reasonable and comparable to the IERS Conventions 2010 model. Even though there are slight punctual improvements using the test model, it is not yet possible to revise the IERS recommended model.

However, there are several possibilities, such as higher spatial resolutions of ocean tide models or the use of (more) minor tides, which may lead to improved high-frequency ERP predictions.

Acknowledgements

The authors would like to thank the Austrian Science Fund for supporting this work within Project SPOT (P24813).

References

1. G. Petit and B. Luzum (eds.). IERS Conventions (2010). (IERS Technical Note; 36) Frankfurt am Main: Verlag des Bundesamts für Kartographie und Geodäsie, 179 pp., ISBN 3-89888-989-6, 2010.
2. H.-P. Plag and M. Pearlman (eds.). Global Geodetic Observing System. 376 pp., ISBN 978-3-642-02687-4, 2009.
3. R. Gross. The effect of ocean tides on the Earth's rotation as predicted by the results of an ocean tide model. In *Geophysical research letter*, Vol. 20, No. 4, pages 293–296, 1993.
4. IHO. Harmonic constituents with Nodal Corrections. Harmonic constants, Product Specification, Edition I, 2006.
5. W. H. Munk and D. E. Cartwright. Tidal Spectroscopy and Prediction. In *Phil. Trans. R. Soc.*, Vol. 259, No. 1105, pages 533–581, 1966.
6. R. D. Ray. Inversion of oceanic tidal currents from measured elevations. In *Journal of Marine Systems*, Vol. 28, pages 1–18, 2001.